Journal of Applied Electrochemistry **34**: 495–500, 2004.

Self-assembly of metalloporphyrin-L-cysteine modified gold electrode

S. WANG[1,*], D. DU[1], X. XU[2]
[1]*Faculty of Chemistry and Material Science, Hubei University, Wuhan, 430062, China*
[2]*Department of Chemistry, Changshu College of Jiangsu, Changshu 215500, China*
*(*author for Correspondence, e-mail: wangsf@hubu.edu.cn)*

Received 19 March 2003; accepted in revised form 19 November 2003

Key words: electrocatalytic reduction, L-cysteine, linear sweep voltammetry, metalloporphyrin, self-assembled monolayers

Abstract

A novel composite film containing metalloporphyrins was fabricated by *in situ* electrochemical scanning on an L-cysteine self-assembled monolayer modified gold electrode. SEM and ATR-FTIR were used to characterize the structure of the film. The electrochemical properties were investigated through techniques such as a.c. impedance, cyclic voltammetry and chronocoulometry. The porphyrin-L-cysteine film showed no peak in the first cycle, while each of the composite films derived from three different metalloporphyrin-L-cysteines presented a pair of reversible redox peaks in 1.0 mol L^{-1} H_2SO_4. These peaks correspond to the rapid redox process of the metal. The supporting electrolyte and its pH value influenced the stability and sensitivity of the composite film. Cupric-porphyrin-L-cysteine film showed good catalytic activity for the reduction of H_2O_2. The catalytic current was linear to H_2O_2 concentration in the range 1.0×10^{-6} to 3.0×10^{-5} mol L^{-1}, with a correlation coefficient of 0.9995. The detection limit was 1.0×10^{-7} mol L^{-1} at a signal to noise ratio of 3. The relative standard deviation was calculated as 2.4% for solutions containing 1.0×10^{-5} mol L^{-1} H_2O_2 ($n = 11$).

1. Introduction

Self-assembled monolayers (SAMs) have become a subject of intense interest in materials science and molecular technologies, because they provide highly ordered structures on surfaces [1]. SAMs with terminal functional groups can be used to construct organic surfaces with a variety of functional properties. SAMs derive their chemical selectivity from the outermost few angstroms of the film and in recent years, there have been many examples of self-assembly and self-organization to rationally synthesize novel functional materials [2]. We have recently demonstrated design strategies for solid-state supramolecular arrays containing both heteropoly-anion-L-cysteine [3] and ferrocene-L-cysteine [4]. Recently, organization of porphyrinic chromophores on thin film organic surfaces through hydrogen bonds provides another powerful means for the design of novel systems with useful functional properties [5]. The strategies to prepare SAMs with porphyrinic chromophores have relied on either the modification of the porphyrin periphery with thiol sidechains [5, 6] or on the coordination of thiols terminating in N-donor heterocycles to metal ions [5, 7] or P-ligand [8] already bonded in the porphyrin cavity. Recently, much attention has been paid to layer-by-layer self-assemblies [9–12] based on electrostatic attraction because they are ideal supramolecular systems. In this communication, we report strategies to link metalloporphyrins to surface-confined monolayers of L-cysteine through electrostatic interaction.

Among the conventional immobilization procedures for metalloporphyrins, only electrochemical deposition offers the possibility of electrogenerating a polymer film precisely over small electrode surfaces of complex geometry. In this context, we describe the adsorption of tetramethoxyphenyl-porphyrin (H_2TMPP) on L-cysteine modified gold electrode and the preparation of ferri-porphyrin (FeTMPP), cupric-porphyrin (CuTMPP), cobaltic-porphyrin (CoTMPP). Attenuated total reflection-Fourier transform infrared (ATR-FTIR), scanning electron microscopy (SEM) and cyclic voltammetry (CV), chronocoulometry (CC) were used to characterize the composite film modified gold electrode. The application for the electrocatalytic reduction and amperometric determination of H_2O_2 was discussed.

2. Experimental details

2.1. *Experimental apparatus*

Electrochemical measurements were carried out on CHI630A (Co. CHI, USA). A three-electrode system was used in the measurements, with a bare gold electrode (dia. 2 mm) or metalloporphyrins-L-cysteine modified gold electrode (NTMPP-L-Cys/Au CME,

N = Fe, Cu, Co) as the working electrode, a saturated calomel electrode (SCE) as the reference and a platinum wire as the auxiliary electrode. All potentials were referred to the SCE. FTIR spectra were recorded on a Vector 22 Fourier transform infrared spectrometer (Bruker) operated in the diffuse reflectance mode at a resolution of 4 cm^{-1}. SEM photographs were obtained with a Hitachi S-570 (Japan). Complex-impedance plots were measured in 1.0×10^{-3} mol L^{-1} $K_4[Fe(CN)_6]$ + 1.0×10^{-3} mol L^{-1} $K_3[Fe(CN)_6]$ + 0.5 M KNO_3 at a bias potential of 0.22 V vs SCE. All experiments were conducted at room temperature.

2.2. *Materials*

H_2TMPP was supplied by Wuhan University (China), $Fe(NO_3)_3$, $Cu(NO_3)_2$, $Co(NO_3)_3$, CH_2Cl_2 and other chemicals were of analytical grade and used without further purification. All solutions were prepared with double-distilled water. Stock solutions of 1.0×10^{-2} mol L^{-1} H_2O_2 were prepared in 0.01 mol L^{-1} HCl.

2.3. *Preparation of NTMPP-L-Cys/Au CME*

To obtain a stable NTMPP-L-Cys/Au CME, L-cysteine, a self-assembled monolayer (L-Cys/Au SAMs) modified gold electrode had to be formulated first. The bare gold electrode was polished to a mirror finish with 0.05 μm α-Al_2O_3 slurry on microcloth pads and then rinsed thoroughly with distilled water. This bare gold electrode was immersed in Piranha solution (a hot mixed solution of 30% H_2O_2 and concentrated H_2SO_4, volume ratio 1:3) for 10 min, followed by sonicating in doubly distilled water and absolute ethanol, respectively. The electrode was voltammetrically cycled and characterized in 1.0 mol L^{-1} H_2SO_4 until a stable cyclic voltammogram was obtained. This freshly pretreated electrode was immersed in 0.05 mol L^{-1} L-cysteine solution for 24 h and then washed thoroughly in an ultrasonic bath with pure water to remove the non-chemisorbed materials. Using this method L-Cys/Au SAMs was obtained. A drop of CH_2Cl_2 solution containing 1.0×10^{-2} mol L^{-1} H_2TMPP was dropped on L-Cys/Au SAMs and dried naturally, in this way a thin film of H_2TMPP was prepared on L-Cys/Au SAMs, which was called H_2TMPP-L-Cys/Au SAMs. Subsequently, it was scanned over several cycles between −0.1 V and 0.8 V at 100 mV s^{-1} in 1.0 mol L^{-1} H_2SO_4 containing 1.0×10^{-2} mol L^{-1} $Fe(NO_3)_3$, $Cu(NO_3)_2$, $Co(NO_3)_3$ separately to prepare FeTMPP-L-Cys/Au CME, CuTMPP-L-Cys/Au CME and CoTMPP-L-Cys/Au CME. Although, the method to prepare metalloporphrins was the same, the preparing process was varied depending upon the metal ion used. To obtain stable composite film, 20 cycles were scanned in FeTMPP-L-Cys/Au CME and 50 cycles in CuTMPP-L-Cys/Au CME while at least 100 cycles were scanned in CoTMPP-L-Cys/Au CME.

3. Results and discussion

3.1. *SEM*

The presence of the L-Cys/Au SAMs film on a gold electrode surface can be confirmed by SEM photograph (Figure 1). In Figure 1(a), showing a bare gold electrode surface, many defects were observed. These pores were due to the preimmersion in Piranha solution, which made the surface of the bare gold much more rough. However, a layer of film of L-Cys/Au SAMs was obtained as shown in Figure 1(b). All these phenomena indicated that L-cysteine molecule has been assembled on the gold surface.

3.2. *Impedance analysis in presence of* $Fe(CN)_6^{3-/4-}$

The a.c. impedance method is based upon a measurement of the response of the electrochemical cell to a

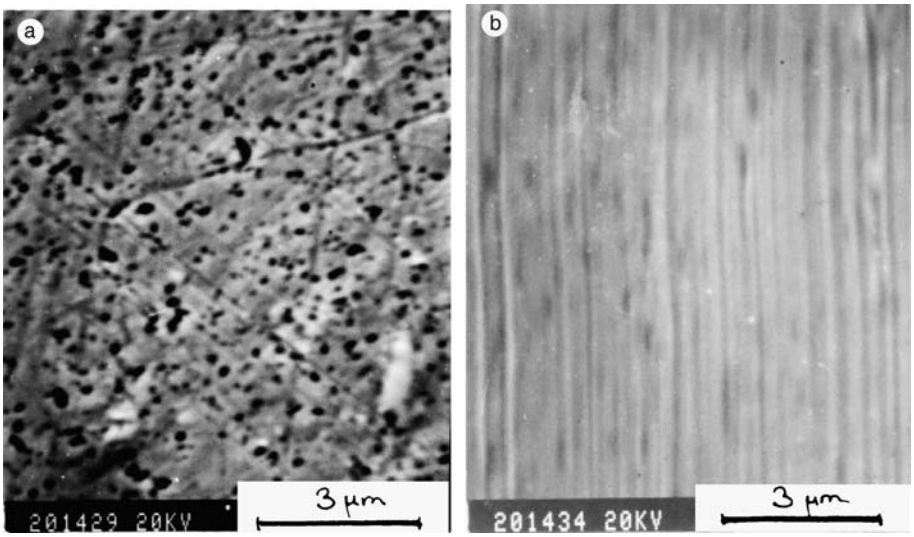

Fig. 1. SEM photographs of bare gold surface (a) and L-Cys/Au SAMs film modified gold surface (b).

small-amplitude alternating potential. The response is often shown as a complex-impedance presentation, and the result can be interpreted in terms of an equivalent electrical circuit. The surface changes of the electrode must cause a change in the a.c. response; this change can be understood according to Randles' equivalent circuit [13], and can be used to estimate the electrode coverage and some kinetic parameters, such as the charge-transfer rate constant, and the dielectric constant of the monolayer film.

In terms of the Randles' equivalent circuit, attention was focused on the more interesting part of the spectrum at high frequency, where the electrode reaction was purely kinetically controlled, and the heterogeneous charge-transfer resistance was expected to increase, due to inhibition of the electron transfer by the monolayer on the electrode surface [14]. The electrode coverage (θ) is a key factor which can be used to estimate the surface state of the electrode, and the charge-transfer resistance is also related to it. Assuming that all the current is passed by pinholes on the electrode, the electrode coverage can be calculated by $(1-\theta) = R_{ct}^0/R_{ct}$ [15], where R_{ct}^0 is the charge-transfer resistance at bare gold and R_{ct} is the charge-transfer resistance at the monolayer-covered electrode under the same conditions.

Figure 2 shows a complex-impedance plot of L-Cys/Au SAMs. Comparison of complex impedance plots for a bare electrode and a monolayer-covered gold electrode showed the effect of the absorbed L-Cys monolayers on the a.c. response. For a monolayer-covered electrode, R_{ct}, which was the diameter of the semicircle at high frequency, was clearly greater than that of the bare electrode due to an inhibition of L-Cys/Au SAMs to electron transfer. The semicircle measured at the bare gold was poorly defined, due to fast electrode reaction, while it was well defined at the monolayer-coated electrode. From an analysis of the spectrum shown in Figure 2, the charge-transfer resistance was 3232 Ω cm^2 and the corresponding electrode coverage was estimated to be 99.4%. The charge-transfer resistance for bare gold was measured as 20.4 Ω cm^2.

3.3. *ATR-FTIR Spectra of H_2TMPP-L-Cys/Au SAMs*

Figure 3 presents the ATR-FTIR spectra of crystalline H_2TMPP and H_2TMPP-L-Cys/Au SAMs. 3314 cm^{-1} of N–H [16] vibration was obvious in the H_2TMPP FTIR spectrum. This appeared at 3311 cm^{-1} in the H_2TMPP-L-Cys/Au SAMs modified gold electrode. In addition, the bands at 1600, 1500 and 1450 cm^{-1} were diagnostic of the benzene ring [16] and the bands between 2800–3000 cm^{-1} were C–H vibration of benzene. All these phenomena showed that H_2TMPP was modified on the electrode surface. The slight shift was probably related to the interaction between H_2TMPP and L-cysteine.

3.4. *Electrochemical behaviour of NTMPP-L-Cys/Au CME*

3.4.1. *Cyclic voltammetric behaviour*

There were no redox peaks in the first cyclic scan of H_2TMPP-L-Cys/Au SAMs in 1.0 mol L^{-1} H_2SO_4, in the potential range 0.0 to 0.8 V (Figure 4). However, two pairs of peaks appeared in 1.0 mol L^{-1} H_2SO_4 (Figure 4(1)). Therefore, the reduction of H_2TMPP takes up $2e^-$ and $2H^+$ in aqueous solution [17, 18]. Accordingly, the reduction mechanism of H_2TMPP on the electrode in aqueous media may be described as follows:

$$(H_2TMPP)_{ss} \rightleftharpoons (TMPP)_{ss} + 2e^- + 2H^+_{aq}$$

However, three NTMPP-L-Cys/Au CME (N = Fe, Cu, Co) gave a pair of reversible redox peaks, respectively, in 1.0 mol L^{-1} H_2SO_4. $E_{pa} = 0.470$ V, $E_{pc} = 0.384$ V (Figure 5); $E_{pa} = 0.304$ V, $E_{pc} = 0.185$ V (Figure 6); $E_{pa} = 0.125$ V, $E_{pc} = 0.001$ V (Figure 7). It was the metal of the metalloporphyrin-L-cysteine composite film that presented redox activity.

Comparing with the CV of H_2TMPP-L-Cys/Au SAMs, the two poor peaks disappeared, which indicated

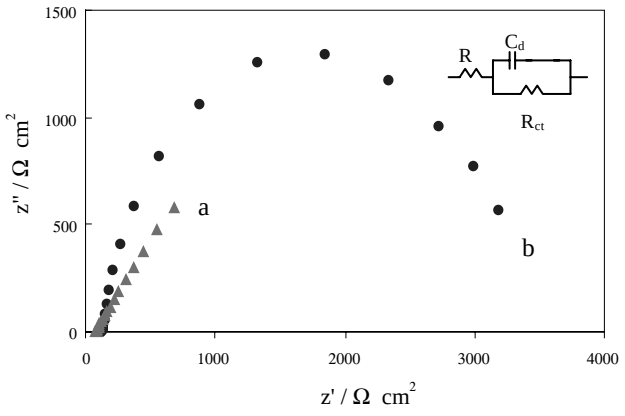

Fig. 2. Complex-impedance plots measured in 1.0 mM $K_4[Fe(CN)_6]$ + 1.0 mM $K_3[Fe(CN)_6]$ + 0.5 M KNO_3 at a bias potential of 0.22 V vs SCE for bare gold electrode (a) and L-Cys/Au SAMs film modified gold surface (b), the frequency range is 0.1–10 000 Hz.

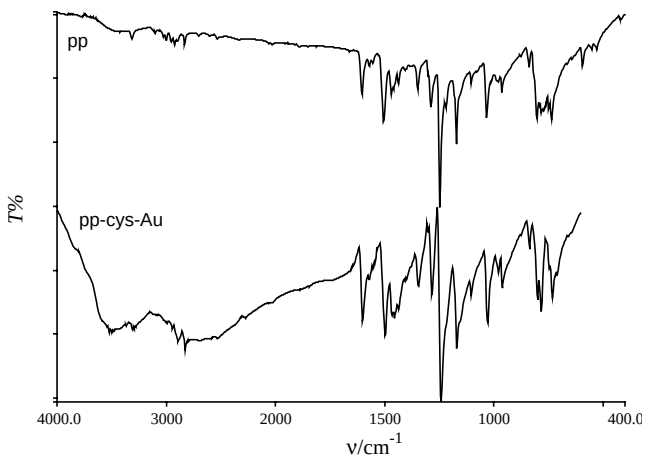

Fig. 3. ATR-FTIR of crystalline L-Cysteine (a), L-Cys/Au SAMs (b).

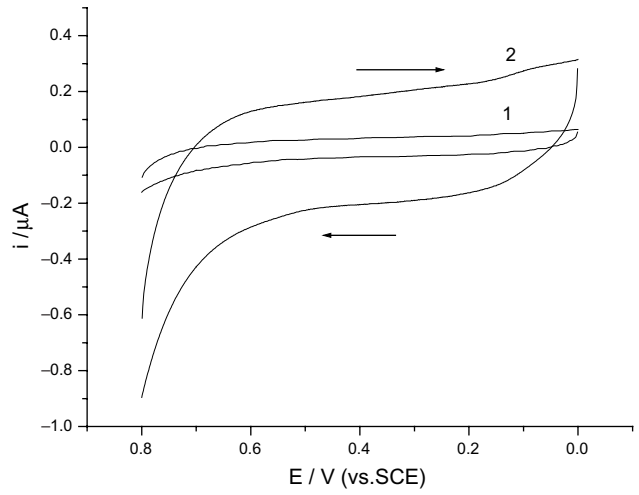

Fig. 4. Background currents of H_2TMPP-L-Cys/Au SAMs (1) and L-Cys/Au SAMs (2).

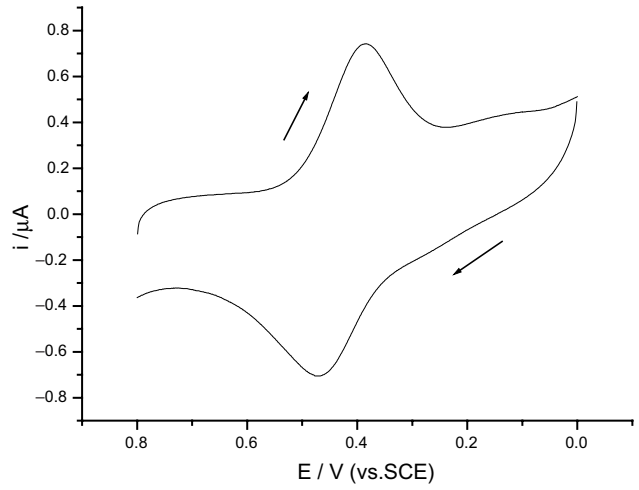

Fig. 5. Cyclic voltammograms of FeTMPP-L-Cys/Au CME in 1.0 mol L^{-1} H_2SO_4. Scan rate: 50 mV s^{-1}.

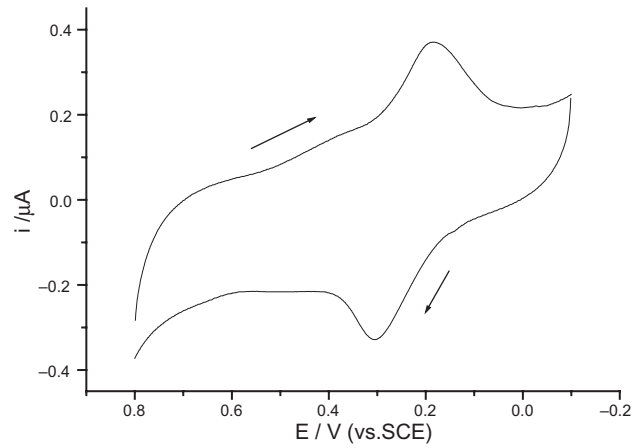

Fig. 6. Cyclic voltammograms of CuTMPP-L-Cys/Au CME in 1.0 mol L^{-1} H_2SO_4. Scan rate: 50 mV s^{-1}.

a rapid redox process of the metal. At lower scan rate (5–50 mV s^{-1}), all the peak potentials remained unchanged and ΔE_p did not increase with scan rate (v). The peak currents (i_p) increased with scan rate and the electrochemical behaviour of three NTMPP-L-Cys/Au CME indicates a diffusion process (i_p proportional to $v^{1/2}$). At higher scan rate (50–200 mV s^{-1}), a good linearity in the plot of i_p/v revealed that the electrochemical behaviour showed an adsorption process. The surface coverage of NTMPP can be calculated from $i_p = n^2F^2vA\Gamma/4RT$, where i_p, v, A, Γ represent the peak current (A), scan rate (V s^{-1}), electrode area (cm^2) and surface coverage of the redox species (mol cm^{-2}), respectively [19]. It indicates monolayer adsorption [20–22].

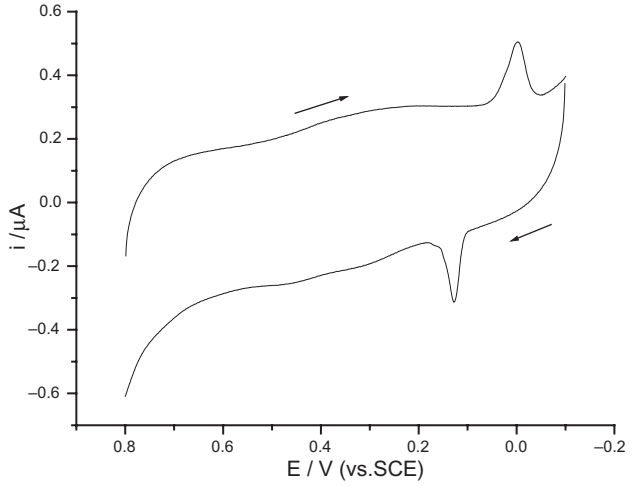

Fig. 7. Cyclic voltammograms of CoTMPP-L-Cys/Au CME in 1.0 mol L^{-1} H_2SO_4. Scan rate: 50 mV s^{-1}.

3.4.2. *Effect of pH on NTMPP-L-Cys/Au CME*

The stability and sensitivity of NTMPP-L-Cys/Au CME was influenced by the pH of the buffer solution. The peak currents decreased and peak potentials shifted negatively. However, there was no redox peak when pH > 3, because metalloporphyrins were unstable at high pH. Considering the sensitivity, we selected 1.0 mol L^{-1} H_2SO_4 as supporting electrolyte. Figure 8 presentes the influence of pH on the behaviour of CuTMPP-L-Cys/Au CME.

3.4.3. *Influence of different supporting electrolyte on NTMPP-L-Cys/Au CME*

NTMPP-L-Cys/Au CME showed the same CV behaviour in 1.0 mol L^{-1} H_2SO_4, HNO_3 and HCl, while giving different CV curves in $NaNO_3$, KNO_3 and NH_4NO_3.

3.5. *Stability of NTMPP-L-Cys/Au CME*

The stability of the electrode was examined by measuring the decrease in voltammetric currents of the composite film electrode during potential cycling. For example, when the film electrode was subjected to 200 potential cycles in the potential range 0.0–0.8 V at 50 mV s^{-1}, a decrease in current of only about 5% was

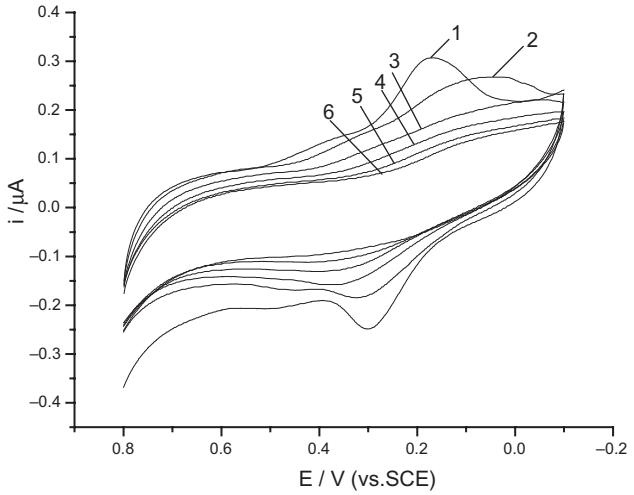

Fig. 8. Effect of pH values on CuTMPP-L-Cys/Au CME (1:1.02; 2:2.03; 3:3.02; 4:4.05; 5:5.03; 6:6.08).

observed. After soaking the NTMPP-L-Cys/Au CME in 1.0 mol L^{-1} H_2SO_4 for at least 24 h, there was no change in the electrochemical response. These experiments showed good stability and high electrochemical activity of NTMPP-L-Cys/Au CME.

3.6. *Electrocatalytic effect of CuTMPP-L-Cys/Au CME on the reduction of H_2O_2*

The reduction of H_2O_2 was totally irreversible at a glassy carbon electrode and a bare gold electrode. However, the reduction of H_2O_2 could readily be catalysed by CuTMPP-L-Cys/Au CME (Figure 9). With the addition of H_2O_2, the cathodic current increased and the corresponding anodic current decreased. These results indicated that CuTMPP-L-Cys/Au CME had catalytic properties toward the reduction of H_2O_2. To improve the sensitivity of the composite film for the quantitative determination of H_2O_2, differential pulse

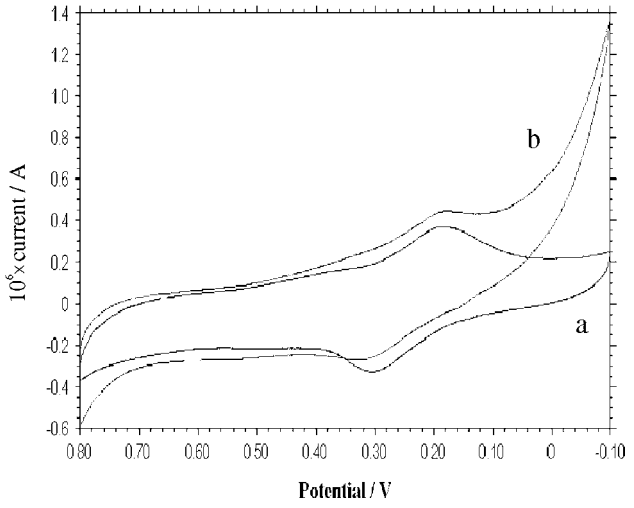

Fig. 9. Electrocatalytic reduction of CuTMPP-L-Cys/Au SAMs to H_2O_2 Cyclic voltammograms of CoTMPP-L-Cys/Au CME in 1.0 mol L^{-1} H_2SO_4 (a), 1.0 mol L^{-1} H_2SO_4 containing H_2O_2 (b).

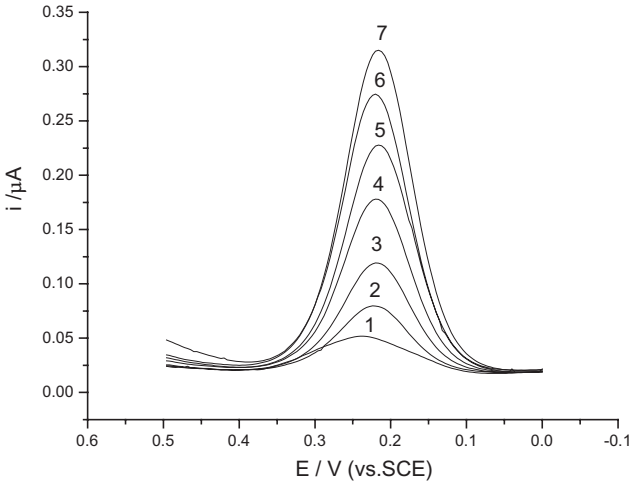

Fig. 10. Determination of H_2O_2 by differential pulse voltammetry at CuTMPP-L-Cys/Au CME in 1.0 mol $L^{-1}H_2SO_4$ 1:3.0; 2:6.0; 3:10; 4:15; 5:20; 6:25; 7:30 μmol L^{-1}.

voltammetry (DPV) was adopted to record the reduction peak current of different concentrations of H_2O_2, as shown in Figure 10. The catalytic current of H_2O_2 against its concentration had a good linear relation in the range 1.0×10^{-6}–3.0×10^{-5} mol L^{-1}. The regression equation was $i_{pa} = 0.01006\ c + 0.02264$ (i_{pa} in μA; c in μmol L^{-1}), with a correlation coefficient of 0.9995. The detection limit (three times the noise) was 1.0×10^{-7} mol L^{-1} and the relative standard deviation was 2.4% for solution containing 1.0×10^{-5} mol L^{-1} H_2O_2 ($n = 11$).

4. Conclusion

A novel composite film containing metalloporphyrins has been fabricated on a L-cysteine self-assembled monolayer modified gold electrode by *in situ* electrochemical scanning. SEM, ATR-FTIR, a.c. impedance, CV and CC showed that H_2TMPP was modified on the electrode surface. The slightly shift was probably related to the interaction between H_2TMPP and L-cysteine. Three NTMPP-L-Cys/Au CME (N = Fe, Cu, Co) gave a pair of reversible redox peaks in 1.0 mol L^{-1} H_2SO_4 and H^+ took part in the redox reaction.

Acknowledgement

This work was financially supported by the Natural Science Foundation of Hubei Province of China (grant 2000J007).

References

1. A. Ulman, *Chem. Rev.* **96** (1996) 1533.
2. K. Itsumaro, A. Akira and O. Masaaki, *J. Fluorine Chem.* **109** (2001) 67.
3. S.F. Wang, D. Du and Q.C. Zou, *J. Anal. Chem.* (Chinese) **30** (2002) 178.

4. S.F. Wang, W. Wang and D. Du, *Anal. Lett*. **35** (2002) 1823.
5. N. Kanayama, T. Danbara and H. Kitano, *J. Phys. Chem. B*. **104** (2000) 271.
6. I. Hiroshi, Y. Hiroko, N. Yoshinobu, Y. Iwa, S. Yoshiteru and M. Vectorial, *J. Phys. Chem. B* **104** (2000) 2099.
7. D.A. Offord, S.B. Sachs, M.S. Ennis, T.A. Eberspacher, J.H. Griffin, C.E.D. Chidsey and J.P. Collman, *J. Am. Chem. Soc*. **120** (1998) 4478.
8. A.L. Bramblett, M.S. Boeckl, B.D. Ratner, T. Sasaki and J.W. Rogers, American Vacuum Society, Seattle, WA, October (1999).
9. A. Kuhn and F.C. Anson, *Langmuir* **12** (1996) 5481.
10. I. Ichinose, H. Tagaua, S. Mizuki and T. Kunitake, *Langmuir* **14** (1998) 187.
11. L. Cheng and S.J. Dong, *J. Electroanal. Chem*. **481** (2000) 168.
12. C.Q. Sun and J.D. Zhang, *Electrochim. Acta* **43** (1997) 943.
13. M. Sluyters-Rehhach and J.H. Sluyters, *in* A.J. Bard (Ed), 'Electroanalytical Chemistry' Vol.4 (Marcel Dekker, New York, 1970).
14. C. Amatore, J.M. Saveant and D. Tessier, *J. Electroanal. Chem*. **147** (1983) 39.
15. E. Sabatani and J. Sagiv, *J. Electroanal. Chem*. **219** (1987) 365.
16. 'The Sadtler Standard Spectra Standard Infrared Grating Spectra. ©1973', Sadtler Research Laboratories, (Subsidiary of Block Engineering, Inc), 28121K.
17. Q.K. Zhuang and X.X. Gao, *Electrochim. Acta* **40** (1995) 959.
18. M.H. Barley, K.J. Takeuchi and T.J. Meyer, *J. Am. Chem. Soc*. **108** (1986) 5876.
19. A.J. Bard and L.R. Faulkner, 'Electrochemical Methods-Fundamentals and Applications' (Chemical Industry Press, Beijing, 1986).
20. X.Y. Hu, Y. Xiao and H.Y. Chen, *J. Electroanal. Chem*. **466** (1999) 26.
21. R.W. Murray, *in* A.J. Bard (Ed), 'Electroanalytical Chemistry' (Marcel Dekker, New York, 1984).
22. J. Wang, B.Z. Zeng, C. Fang and X.Y. Zhou, *Electroanalysis* **12** (2000) 763.